Phase and energy distribution of ions incident on electrodes in radio-frequency discharges

Gregory A. Hebner and Mark J. Kushner
Gaseous Electronics Laboratory, Department of Electrical and Computer Engineering, University of Illinois at Urbana-Champaign, 607 East Healey, Champaign, Illinois 61820

(Received 13 April 1987; accepted for publication 11 June 1987)

A Monte Carlo particle simulation and parametric models for the sheath voltage and thickness were used to calculate the arrival phase and energy of ions striking the electrodes in low-pressure capacitively coupled rf discharges. Ion phase and energy distributions are presented as a function of rf frequency, ion mass, rf voltage, dc bias, sheath thickness, and gas pressure. When the rf frequency is below the ion response frequency, the ions arrive at the electrode in phase with the applied rf voltage. As the rf frequency increases, the highest ion arrival probability shifts towards higher phase until, at sufficiently high frequencies, it is nearly uniform. The transition from a highly peaked ion phase distribution at low frequencies to a uniform distribution at high frequencies requires at least an order of magnitude change in rf frequency. The implication of these calculations on the electron energy distribution is discussed.

I. INTRODUCTION

Low-pressure radio-frequency (rf) discharges are now commonly used for plasma processing of semiconductor materials.[1,2] In order to predict the characteristics of the plasma reactor and the materials produced, studies have been performed of the electron kinetics in such systems.[3–13] The results of theoretical[3–5] and experimental[6–12] investigations have indicated that the electron energy distribution is a function of space and time. In general, the majority or "bulk" of the electron energy distribution is composed of low-energy electrons with a small "tail" of high-energy electrons. The high-energy tail of the distribution results from secondary electrons produced by ion bombardment which are accelerated by the sheath potential, and from the acceleration of bulk electrons by the oscillating sheath boundary. Since a portion of the high-energy tail of the electron energy distribution is the result of ion bombardment, knowing the time and energy distributions of the ions striking the electrode is important to accurately describe the temporal and spatial behavior of the tail of the electron energy distribution. In this paper we report on a theoretical investigation of the time and energy dependence of ions bombarding the electrodes in a low-pressure rf discharge. Previous studies of ion bombardment of the electrodes in rf discharges have only examined the distribution of energies or angles of the ions that strike the electrode.[9–13] As a result, the main emphasis of this study is the investigation of the arrival time, or phase of the ions with respect to the applied rf voltage, and the energy distribution of the ions that strike the electrode after traversing the sheath.

The model is described in Sec. II, followed by a discussion of the results for frequency, ion mass, voltage, and sheath thickness in Sec. III. Concluding remarks are in Sec. IV.

II. DESCRIPTION OF THE MODEL

The study was performed using a Monte Carlo simulation similar to that previously described.[13] Therefore, the model will only be discussed briefly. The voltage drop across the sheath and the sheath thickness are assumed to have the form

$$V(t) = \max(V_{dc} + V_{rf} \sin \omega_{rf} t, V_{min}) \quad (1)$$

and

$$l(t) = \max(X_{dc} + X_{rf} \sin \omega_{rf} t, X_{min}) , \quad (2)$$

where $V(t)$ is the time dependent voltage across the sheath, $l(t)$ is the sheath thickness, and ω_{rf} is the rf frequency. The subscripts on V and X denote to the time-independent (dc) and the time-dependent (rf) components of the applied voltage and sheath thickness, respectively. max (a,b) indicates the maximum value of a or b. As our concern is with electropositive plasmas where the plasma potential is always positive, the function max is used to guarantee a positive sheath potential. V_{min} and X_{min} as equal to 0.001. The spatial distribution of the electric field within the sheath is chosen to be linear and has the form

$$E(x,t) = E_0[l(t) - x] , \quad (3)$$

where

$$E_0 = 2[V(t)/l(t)] . \quad (4)$$

Using the above parametric models, the trajectories of the ions in the sheath are computed using standard Monte Carlo techniques.[14,15] The ions are injected into the simulation with a random velocity chosen from a Maxwellian distribution. Their initial spatial positions are greater than the maximum sheath thickness $(X_{dc} + X_{rf})$. As previously described,[13] elastic and charge exchange collisions are included in the simulation by specifying a mean free path λ, and randomly choosing a collision distance l_c, such that

$$l_c = -\lambda \ln(r) , \quad (5)$$

where r is a random number on $(0,1)$. When the ions strike the electrode, their energy and arrival time with respect to the applied rf voltage are recorded.

Simulations were performed in helium and argon for frequencies in the range of 0.1–40.0 MHz, rf voltages of 400–

 0021-8979/87/182256-05$02.40

800 V, dc biases of 0–300 V, gas densities of 1.0×10^{16}–5.0×10^{16} cm^{-3} and sheath thicknesses of 0.5–1.5 cm.

III. RESULTS AND DISCUSSION

Unless noted otherwise, the discharge conditions for the simulation of helium and argon ions striking the electrodes were a peak rf voltage (V_{rf}) of 400 V, maximum sheath thickness (X_{rf}) of 0.5 cm, and gas density of 1.0×10^{16} cm^{-3}. The dc bias (V_{dc}) and the time-independent sheath thickness (X_{dc}) were set to zero for the first cases discussed below. For the calculations in helium, an energy-independent charge exchange collision cross section of 1.5×10^{-15} cm^2 and an elastic collision cross section of 1.0×10^{-16} cm^2 were used. We found that the results were insensitive to the choice of the elastic collision cross section as long as $\sigma_{elastic} \ll \sigma_{charge\ exchange}$. The calculations with argon ions were performed with energy-independent charge exchange and elastic collision cross sections of 2.5×10^{-15} cm^2. For both gases, the initial ion velocity was chosen to be close to the Bohm criterion for an electron temperature of 10 000 K. Trials showed that variation of the initial ion velocity had a very small effect on the final distributions. Good statistics were obtained with runs of 10 000 particles.

A. rf frequency and ion mass

The dependence of the ion energy distribution and the arrival phase at the electrode of light and heavy ions is shown in Figs. 1–4. Figures 1 and 2 show the distribution of arrival times for He ions and Ar ions as a function of frequency and phase with respect to the rf cycle. A phase of 0–π represents the cathodic part of the cycle, while a phase of π–2π denotes the anodic part of the cycle. We define a parameter, the ion response frequency, $\omega_I = 1/\tau$, where τ is the time required for the ion to cross the sheath while being accelerated by the average sheath potential. The parameter ω_I for He and Ar ions are approximately 3.6 and 0.76 MHz, respectivly. For low rf frequencies, that is frequencies that are significantly

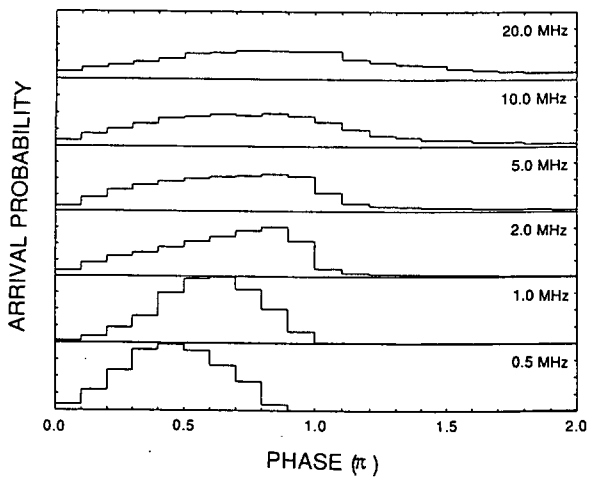

FIG. 1. Relative total arrival probability of He ions striking the electrodes as a function of phase and rf frequency for a peak rf voltage of 400 V, maximum sheath thickness of 0.5 cm, and a pressure of 0.3 Torr. A phase of 0 to π represents the cathodic part of the cycle.

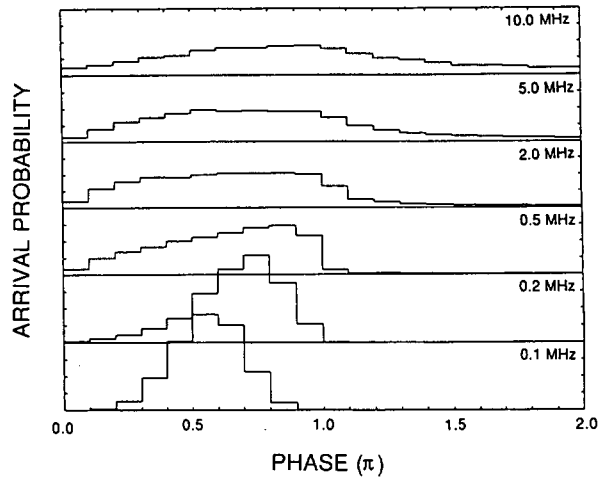

FIG. 2. Relative total arrival probability of Ar ions striking the electrodes as a function of phase and rf frequency for the conditions listed in Fig. 1.

below ω_I, the ions 'follow" the applied rf voltage with the majority of the ions arriving in phase with the voltage. The probability of ions arriving at the electrode during the anodic part of the cycle is small since the sheath region is swept free of ions during the cathodic part of the cycle. Ions must then diffuse into the sheath region from the plasma.

As the frequency increases, the phase of the highest ion arrival probability shifts towards higher phase since the ions no longer have sufficient time, during a single rf cycle, to be accelerated and traverse the sheath in phase with the voltage. At sufficiently high rf frequency, ions, due to their finite mass, can no longer respond to the time varying field but instead respond to a time-averaged field. As a result, the ions tend towards a uniform distribution. However, even at frequencies much higher than ω_I, the ion distribution is not uniform but is skewed towards the cathodic portion of the

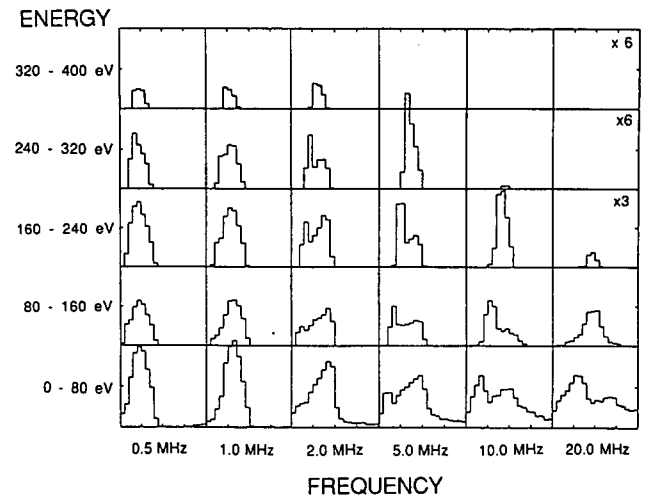

FIG. 3. Relative arrival probability of He ions striking the electrodes as a function of phase, energy range, and rf frequency for the conditions listed in Fig. 1. Within each small block the horizontal axis is phase from 0 to 2π, while the vertical axis is relative arrival probability. The higher energy ranges have been multiplied by a display factor of 3 or 6.

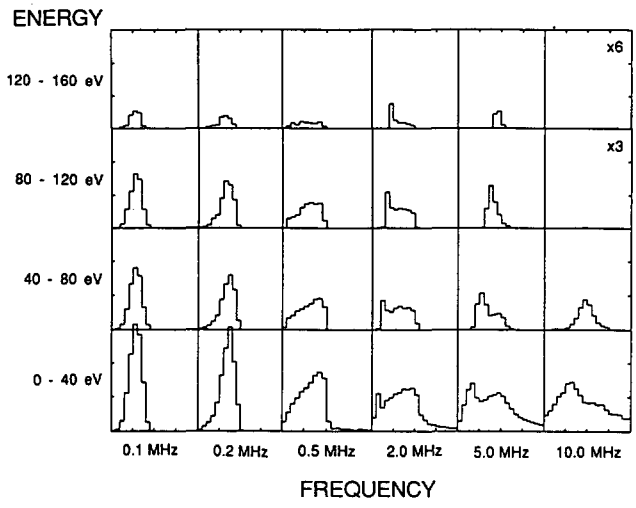

FIG. 4. Relative arrival probability of Ar ions striking the electrodes as a function of phase, energy range, and rf frequency for the conditions listed in Fig. 1. Within each small block the horizontal axis is phase from 0 to 2π, while the vertical axis is relative arrival probability. The higher energy ranges have been multiplied by a display factor of 3 or 6.

cycle. The transition from a peaked behavior at low frequencies to a quasiuniform distribution at high frequencies does not happen rapidly, as illustrated in Fig. 5. The transition requires at least an order of magnitude in rf frequency.

As noted, the high-energy tail of the electron energy distribution is influenced by the ion bombardment of the electrode because of the production of secondary electrons which are then accelerated across the sheath potential. As the peak of the ion phase distribution moves towards higher phase, the production of high-energy secondary electrons will also move towards higher phase. Since the tail of the distribution is responsible for the optical excitation in the He rf discharge,[6] the optical emission from the discharge should show some shift with increasing frequency. This predicted phase shift of a portion of the high-energy tail of the electron energy distribution is suggested by recent experimental results using a high speed framing camera.[6] The time-dependent optical emission from a rf discharge has also been observed using an apertured photomultiplier tube (PMT) and an interference filter (Fig. 6). These results show that at low (0.4 MHz) frequencies, the optical emission peaks during the cathodic half cycle and is approximately in phase with the applied rf voltage. During the anodic half cycle the optical emission is small. At higher frequencies (2.5 MHz), the peak optical emission has moved towards higher phase. These results indicate that the arrival time of the ions on the electrode and the subsequent production of high-energy electrons is phase- and frequency-dependent and that this can have an influence on the discharge kinetics.

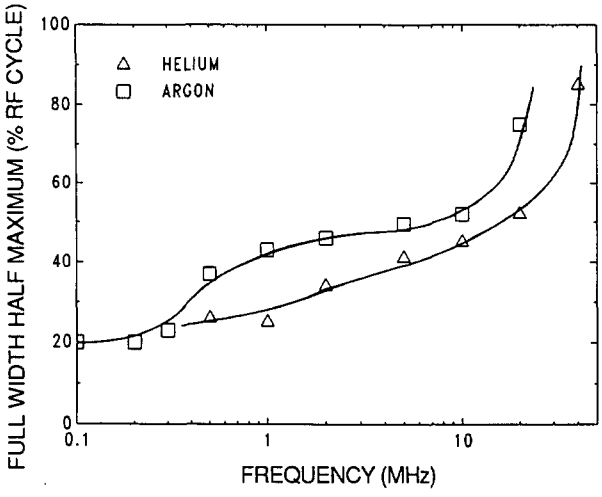

FIG. 5. Measured full width at half maximum of the relative total arrival probabilities shown in Figs. 1 and 2.

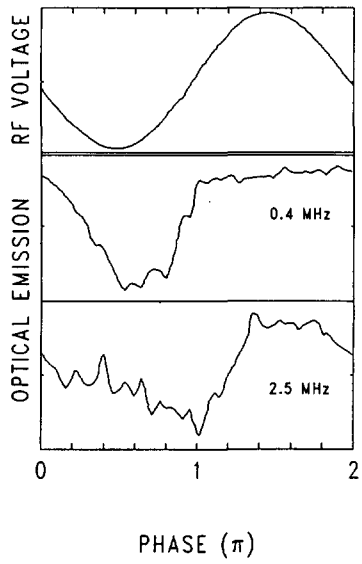

FIG. 6. Optical emission (5875 A, $\tau = 14$ ns) 1 cm below the rf driven electrode in a 0.5-Torr He rf discharge at two frequencies. The rf voltage on the driven electrode is as shown. The negative dc self bias was $\simeq 0$ V for 0.4 MHz and $\simeq 1/3$ the zero to peak voltage for 2.5 MHz. Increasing optical emission is plotted downward. The electrode seperation is 15 cm. The rf circuit is described in Ref. 6. At 0.4 MHz the optical emission peaks approximately in phase with the cathodic portion of the applied rf voltage. At 2.5 MHz, the peak emission is shifted to higher phase. The optical emission at 2.5 MHz is longer due to the negative dc self-bias.

The energy distributions of the helium and argon ions striking the electrodes for the conditions of Fig. 1 are shown in Figs. 3 and 4. Each small plot in Figs. 3 and 4 represents a different energy range (stacked vertically) and rf frequency (horizontal). Within each small plot the horizontal axis is phase from 0–2π and the vertical axis is the probability of an ion arriving at that phase within that energy range.

As previously discussed, for low frequencies, the ions track the rf voltage. Those ions that arrive during the cathodic part of the cycle have a peak in the ion distribution at a phase of approximately $\pi/2$, independent of their energy bin. In addition, those ions which diffuse in from the plasma or are left outside the sheath region when the sheath retreats to the electrode are collected during the anodic part of the cycle with low energy, since the electric field is small. As the rf frequency increases, both the high- and low-energy ion distributions tend to shift toward higher phase. However, the higher energy ions shift towards π and subsequently degrade to lower energy since the ions can no longer follow the field and acquire the maximum sheath potential. Those ions with high velocities during the anodic half cycle rapidly lose their energy through charge exchange collisions and populate the lower energy bins. A decrease in the peak ion energy above ω_I has been observed in chlorine rf discharges.[12] The ion distribution in the lowest energy bin tends to spread out and become more uniform over the entire rf cycle as a consequence of the ions now responding to a quasitime averaged sheath voltage. The end result is that the average ion energy

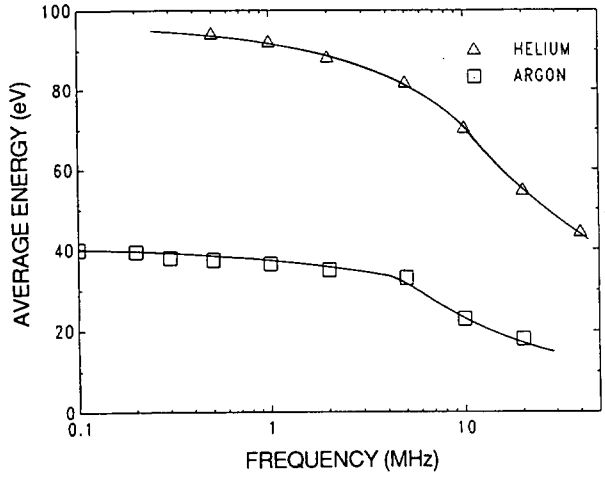

FIG. 7. Average ion energy as a function of rf frequency for He and Ar ions striking the electrodes. Conditions are as described in Fig. 1.

slowly decreases with increasing frequency until a frequency approximately equal to a few ω_i when the ions can no longer track the sheath field. At that point the average energy falls more rapidly (Fig. 7).

The effect of the ion mass (or ω_I) can be observed by comparing Figs. 1 and 3 with Figs. 2 and 4. The frequency when the ions no longer follow the rf frequency is much lower in argon when compared to helium. In both gases the ion phase distributions follow the rf cycle at low frequency, with the most probable arrival time moving towards higher phase and spreading out with increasing rf frequency. However, while the frequencies where the average energy drops off and the ion phase distribution becomes more uniform in time are very different (Fig. 7), they nevertheless scale as ω_I.

B. rf voltage and dc bias

Increasing the rf voltage across the sheath from 400 to 800 V resulted in a linear increase of the average ion energy striking the electrode (Fig. 8). The probability distribution of ion arrival phase changed only slightly with increasing rf voltage. In general, there is a small increase in the height of the ion distribution peak (20%) at the expense of the ions that would normally arrive before the peak. In addition, the absolute position of the peak shifted slightly (less than $\pi/10$) towards the beginning of the cycle. Over this range of rf voltage, only the average energy appears to significantly differ. Thus, the linear relation between average energy and sheath voltage appears to be a valid and useful scaling law.

The effect of imposing a dc voltage and a dc sheath on the ion phase distribution and the average energy was also investigated. For these calculations, the dc voltage and sheath thickness were assumed to scale linearly with the rf voltage and sheath thickness. For example: with $V_{rf} = 400$ V and $X_{rf} = 0.5$ cm, if $V_{dc} = 200$ V, then $X_{dc} = 0.25$ cm. Using this assumption, the ion phase distributions were calculated for He ions, as shown in Fig. 9.

When the dc bias and dc sheath are increased, the ion distribution begins to take on the characteristics of both a rf system with its distinctly peaked behavior and a dc system, where the ion flux is constant in time. With larger bias, the peak becomes smaller and more ions are collected during what was the anodic part of the cycle. However, even though the distribution becomes more uniform with increasing dc bias, the average energy only increases by approximately 10%. This is likely a result of the competing processes of an increased sheath voltage raising the average energy while an increased sheath thickness decreases the average energy due to an increased probability for charge exchange collisions (to be discussed in Sec. III C). The same behavior was also observed for Ar ions.

C. Sheath thickness and pressure

Increasing the rf sheath thickness and the pressure did not have a large effect on the ion phase distribution. With increasing sheath thickness (0.5–1.5 cm) and pressure (1.0×10^{16}–5.0×10^{16} cm^{-3}), the peak height decreased by

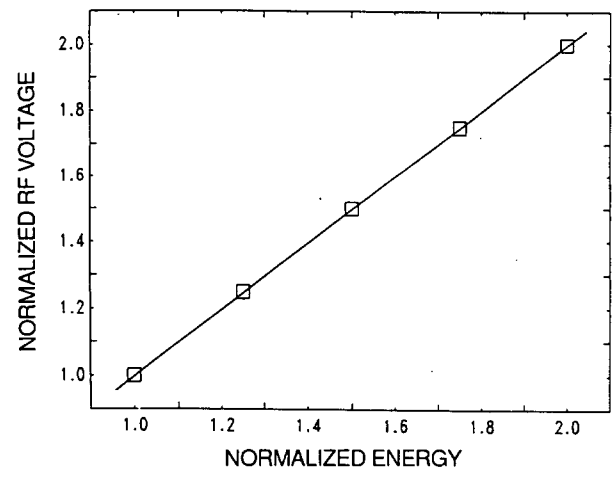

FIG. 8. Normalized He ion energy as a function of rf voltage normalized to 400 V. The ion energy is normalized to the 88.4 eV average energy obtained with a sheath potential of 400 V. The rf frequency is 2.0 MHz.

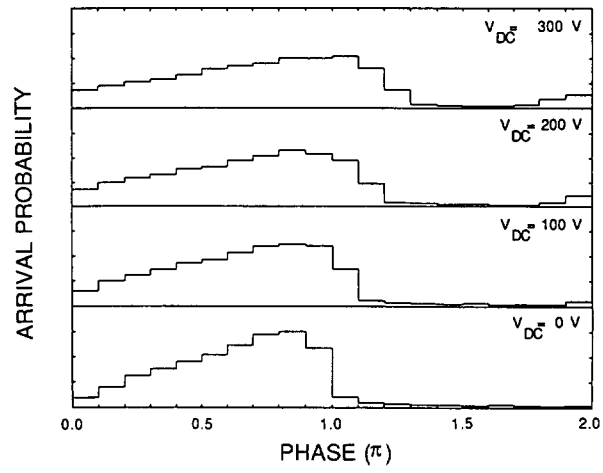

FIG. 9. Relative total arrival probability of He ions striking the electrode with an increasing dc bias and dc sheath thickness. The dc sheath thickness is assumed to increase linearly with increasing dc bias. The rf frequency is 2.0 MHz.

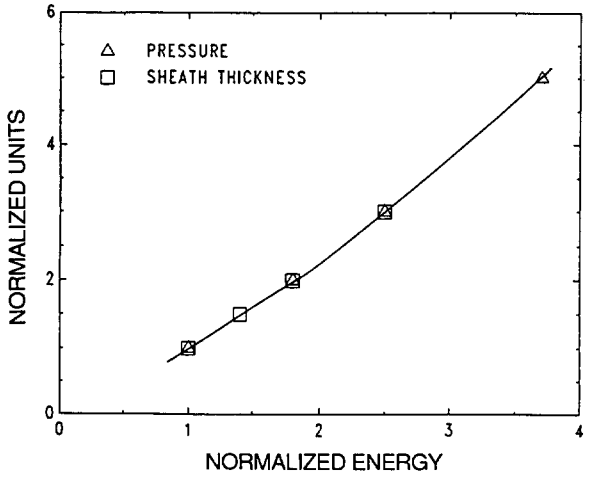

FIG. 10. Normalized He ion energy as a function of the reciprocal of the normalized pressure and sheath thickness. The ion energy is normalized to the 88.4 eV average ion energy in a 2.0 MHz discharge.

15% and 10%, respectively, with a resulting increase in the number of ions arriving before the peak of the distribution. In both cases the absolute position of the phase peak remained in approximately the same position. However, as stated previously, the average ion energy increased approximately linearly with respect to the reciprocal of the sheath thickness and pressure (Fig. 10). The high-energy tail dropped off quickly with increasing sheath thickness and pressure due to an increased number of charge exchange collisions.

IV. CONCLUSIONS

Parametric models for the sheath voltage and thickness and a Monte Carlo particle simulation were used to compute the arrival phase and energy of ions striking the electrodes in low pressure rf discharges. When the rf frequency is below the ion response frequency, the ions arrive at the electrode in phase with the applied rf voltage. As the rf frequency increases, the phase of the highest ion arrival probability shifts towards higher phase and the ion energy decreases. The optical emission from the plasma was also observed to peak approximately in phase with the applied rf voltage at low frequencies. At higher frequencies, the peak optical emission moves to higher phase. The transition from a highly peaked ion distribution at low frequencies to a uniform distribution at higher frequencies required at least an order of magnitude change in rf frequency. Increasing the ion mass or decreasing ω_I decreased the ion energy and reduced the frequency at which the phase distribution tends towards uniform. Increasing the rf voltage linearly increased the average ion energy, while the sheath thickness and pressure are approximately linearly related to the reciprocal of the average energy. Imposing a dc bias on the electrode produced a superposition of a peaked (rf) distribution and a more uniform (dc) ion distribution with little change in average ion energy. Changing the rf voltage, sheath thickness and pressure had only a small effect on the shape of the ion phase distribution.

ACKNOWLEDGMENTS

This work was partially supported by the Materials Science Division of the Army Research Office under the direction of Dr. Andrew Crowson, DAAG29-85-C-0031. One of us (G.A.H.) would like to acknowledge a research fellowship provided by the Army Advanced Construction Technology Center. The authors would like to thank Dr. Joseph Verdeyen for his comments.

[1]D. J. Flamm, V. M. Donnelly, and D. E. Ibbotson, J. Vac. Sci. Technol. B **1**, 23 (1983).
[2]B. Chapman, *Glow Discharge Processes* (Wiley, New York, 1980).
[3]M. J. Kushner, J. Appl. Phys. **54**, 4958 (1983).
[4]D. B. Graves and K. F. Jensen, IEEE Trans. Plasma Sci. **PS-14**, 78 (1986).
[5]A. Garscadden, Mater. Res. Soc. Symp. Proc. **68**, 127 (1986).
[6]G. A. Hebner and J. T. Verdeyen, IEEE Trans. Plasma Sci. **PS-14**, 132 (1986).
[7]D. L. Flamm and V. M. Donnelly, J. Appl. Phys. **59**, 1052 (1986).
[8]R. A. Gottscho, R. H. Burton, D. L. Flamm, V. M. Donnelly, and G. P. Davis, J. Appl. Phys. **55**, 2707 (1984).
[9]B. F. Thompson, K. D. Allen, A. D. Richards, and H. H. Sawin, J. Appl. Phys. **59**, 1890 (1986).
[10]K. Kohler, J. W. Coburn, D. E. Horne, E. Kay, and J. H. Keller, J. Appl. Phys. **57**, 59 (1985).
[11]V. A. Godyak and A. S. Khanneh, IEEE Trans. Plasma Sci. **PS-14**, 112 (1986).
[12]V. M. Donnelly, D. L. Flamm, and R. H. Bruce, J. Appl. Phys. **58**, 2135 (1985).
[13]M. J. Kushner, J. Appl. Phys. **58**, 4024 (1985).
[14]S. L. Lin and J. N. Bardsley, J. Chem. Phys. **66**, 435 (1977).
[15]J. Lucas, Int. J. Electron. **32**, 393 (1972).